Cell Death and Differentiation (2005) 12, 415–428

www.nature.com/cdd

PGE_2 in the regulation of programmed erythrocyte death

PA Lang[1], DS Kempe[1], S Myssina[1], V Tanneur[1], C Birka[1], S Laufer[2], F Lang*[,1], T Wieder[1] and SM Huber[1]

[1] Department of Physiology, University of Tübingen, Germany
[2] Institute of Pharmacy, University of Tübingen, Germany
* Corresponding author: F Lang, Physiologisches Institut der Universität Tübingen, Gmelinstr. 5, D-72076 Tübingen, Germany. Tel: +49 7071 29 72194; Fax: +49 7071 29 5618; E-mail: florian.lang@uni-tuebingen.de

Received 05.4.04; revised 15.11.04; accepted 23.11.04; published online 04.3.05
Edited by M Piacentini

Abstract

Hyperosmotic shock, energy depletion, or removal of extracellular Cl^- activates Ca^{2+}-permeable cation channels in erythrocyte membranes. Subsequent Ca^{2+} entry induces erythrocyte shrinkage and exposure of phosphatidylserine (PS) at the erythrocyte surface. PS-exposing cells are engulfed by macrophages. The present study explored the signalling involved. Hyperosmotic shock and Cl^- removal triggered the release of prostaglandin E_2 (PGE_2). In whole-cell recording, activation of the cation channels by Cl^- removal was abolished by the cyclooxygenase inhibitor diclophenac. In FACS analysis, phospholipase-A_2 inhibitors quinacrine and palmitoyltrifluoromethyl-ketone, and cyclooxygenase inhibitors acetylsalicylic acid and diclophenac, blunted the increase of PS exposure following Cl^- removal. PGE_2 (but not thromboxane) induced cation channel activation, increase in cytosolic Ca^{2+} concentration, cell shrinkage, PS exposure, calpain activation, and ankyrin-R degradation. The latter was attenuated by calpain inhibitors-I/II, while PGE_2-induced PS exposure was not. In conclusion, hyperosmotic shock or Cl^- removal stimulates erythrocyte PS exposure through PGE_2 formation and subsequent activation of Ca^{2+}-permeable cation channels.

Cell Death and Differentiation (2005) **12,** 415–428.
doi:10.1038/sj.cdd.4401561
Published online 4 March 2005

Keywords: cell volume; annexin; osmotic cell shrinkage; glucose depletion; calcium

Abbreviations: PGE_2, prostaglandin E_2; PS, phosphatidylserine; FACS, fluorescence activated cell sorting; *t*-BHP, *t*-butylhydroxyperoxide; PLA_2, phospholipase A_2; COX, cyclooxygenase; PACOCF3, palmitoyltrifluoromethyl ketone; AACOCF3, arachidonyltrifluoromethyl ketone; NMDG, *N*-methyl-D-glucamine; EIPA, ethylisopropylamiloride; MAP kinases, mitogen-activated protein kinase; HEPES, 32-*N*-2-hydroethylpiperazine-*N*-2-ethanesulfonic acid; EGTA, ethylene glycol-bis (β-aminoethyl ether)-*N,N,N′,N′*-tetraacetic acid; EDTA, ethylenediamine -*N,N,N′,N′*-tetraacetic acid; DMSO, dimethyl sulfoxide; PBS, phosphate-buffered saline; FITC, fluorescein isothiocyanate; WGA, *Triticum vulgare* lectin; FSC, forward scatter; SSC, sideward scatter; PMSF, phenylmethylsulfonyl fluoride; SDS, sodium dodecylsulfate; BSA, bovine serum albumin; SDS-PAGE, sodiumdodecylsulfate polyacrylamide gel electrophoresis; ECL, enhanced chemiluminescence

Introduction

Until recently, erythrocytes have been considered unable to undergo apoptosis, as they lack mitochondria and nuclei, key organelles in the apoptotic machinery of nucleated cells.[1] However, most recent observations revealed that treatment of erythrocytes with the Ca^{2+}-ionophore ionomycin leads to cell shrinkage, cell membrane blebbing and annexin binding,[2–7] all typical features of apoptosis in other cell types.[1,8] The breakdown of phosphatidylserine asymmetry results from the activation of a scramblase which is activated by increase of cytosolic Ca^{2+} activity.[9,10] As macrophages are equipped with receptors specific for phosphatidylserine,[11–13] erythrocytes exposing phosphatidylserine at their surface will be rapidly recognized, engulfed and degraded.[14–16] Thus, an increase of cytosolic Ca^{2+} activity could trigger apoptotic death and clearance of erythrocytes.

Ca^{2+} entry further activates Ca^{2+}-sensitive K^+ channels,[17,18] leading to or augmenting cell shrinkage.[19] Ca^{2+} may enter erythrocytes through Ca^{2+}-permeable cation channels,[20,21] which are activated following removal of external Cl^-, osmotic shock by increase of extracellular osmolarity, oxidative stress by addition of *t*-butylhydroperoxide (*t*-BHP) and energy depletion by removal of extracellular glucose.[5,6] Activation of those channels triggers breakdown of phosphatidylserine asymmetry and subsequent erythrocyte death through increased Ca^{2+} leakage into the cell.[5,6] Accordingly, erythrocyte death induced by oxidative stress, energy depletion or removal of external Cl^- was abrogated and hyperosmotic shock-induced erythrocyte death was blunted when the cells are suspended in medium with low free Ca^{2+} concentrations.[5,6] The signalling pathways leading to the activation of the cation channels remained, however, elusive.

Subnanomolar concentrations of prostaglandin E_2 (PGE_2) reportedly lead to activation of erythrocyte cation channels,[22] increase in cytosolic Ca^{2+} concentration,[23] Gardos K^+ channel activation, erythrocyte shrinkage and increased erythrocyte filterability.[24,25] Thus, the present experiments have been performed to explore the involvement of phospholipase A_2 (PLA_2) and cyclooxygenase (COX) in the mechanisms linking osmotic cell shrinkage, removal of Cl^-, and energy depletion to the activation of the cation channels. It is anticipated that this signalling may be important for properties and survival of circulating erythrocytes.

Results

As disclosed by FACS analysis, some 10% of the erythrocytes ($13\pm2\%$; $n=8$) incubated in isotonic NaCl Ringer exhibited reduced wheat germ lectin (agglutinin) binding (Figure 1a, b) as a measure of progressive erythrocyte aging.[26] Among those cells, a significantly higher percentage of erythrocytes bound annexin ($3.5\pm0.5\%$; $n=8$) as compared to (younger) cells with high lectin binding ($1.3\pm0.2\%$; $n=8$; Figure 1c–e). These data point to the presence of distinct erythrocyte subpopulations which differ in their susceptibility to programmed cell death. An increase of extracellular osmolarity to 850 mOsm by addition of 550 mM sucrose to NaCl Ringer was followed by a sharp increase of the percentage of annexin-binding erythrocytes (Figure 2a, left and middle and Figure 2b). This increase was significantly blunted in the presence of the non-specific PLA_2 inhibitor quinacrine (25 μM; Figure 2a, right, and Figure 2b). The inhibitory effect of quinacrine on hyperosmotic shock-induced annexin binding was reversed following coincubation with arachidonic acid (1 μM, Figure 2c). Addition of arachidonic acid (1 μM) alone did not induce significant annexin binding in isotonic extracellular fluid (Figure 2c) and did not significantly enhance the increase of annexin binding following hyperosmotic shock (Figure 2c), suggesting that hyperosmotic shock interferes with the signalling cascade downstream from PLA_2.

Replacement of Cl^- by gluconate similarly triggered annexin binding (Figure 2d–g). The percentage of annexin binding cells upon 48 h extracellular Cl^- removal was variable between the individual experiments (5–57% annexin binding) and averaged to $25\pm3\%$ ($n=30$). Cl^- -removal-induced annexin binding was again sensitive to quinacrine (25 μM; Figure 2d) and inhibited by the cyclooxygenase blockers acetylsalicylic acid (50 μM; Figure 2e) and diclofenac (10 μM; Figure 2f). Moreover, palmitoyltrifluoromethyl ketone (PACOCF3; 4 μM), an inhibitor of the Ca^{2+}-independent PLA_2,[27] blocked about 50% of the Cl^- removal-triggered annexin binding (Figure 2g), while arachidonyltrifluoromethyl ketone (AACOCF3; 8 μM), an inhibitor of the cytosolic PLA_2, had no effect (percentages of annexin-binding cells under control and Cl^--free conditions were 8 ± 1 and $31\pm7\%$ in the presence of AACOCF3 and 6 ± 2 and $30\pm6\%$ in its absence, respectively; means $\pm$ S.E., $n=4$). Higher concentrations of AACOCF3 themselves induced annexin binding of human erythrocytes (data not shown).

Similar to its effect on phosphatidylserine exposure upon hyperosmotic shock or Cl^- removal, quinacrine (25 μM) blunted the annexin binding induced by energy depletion (Figure 2h). In sharp contrast, ionomycin (1 μM)-triggered annexin binding was not sensitive to quinacrine (25 μM; Figure 2i). Taken together, the experimental evidence strongly suggests the involvement of Ca^{2+}-independent PLA_2 and COX in programmed erythrocyte death triggered by osmotic shock or Cl^- removal.

Both experimental manoeuvres, hyperosmotic shock and Cl^- removal, indeed stimulated erythrocyte PGE_2 release as assessed by competitive ELISA. Hypertonic shock (Figure 3a) or Cl^--removal (Figure 3b, c) significantly increased the PGE_2 concentration in the supernatant of erythrocytes within 1 h (850 mOsm) and 3 h (Cl^--free) of incubation. Under both conditions, the PGE_2 concentrations in the supernatant remained two- to four-fold enhanced throughout the 6 h of observation (Figure 3a, b). The Ca^{2+} ionophore ionomycin (1 μM for 1 h) did not stimulate erythrocyte PGE_2 release (Figure 3d). Furthermore, hypertonic shock-stimulated PGE_2 release (850 mOsm for 1 h) was not dependent on

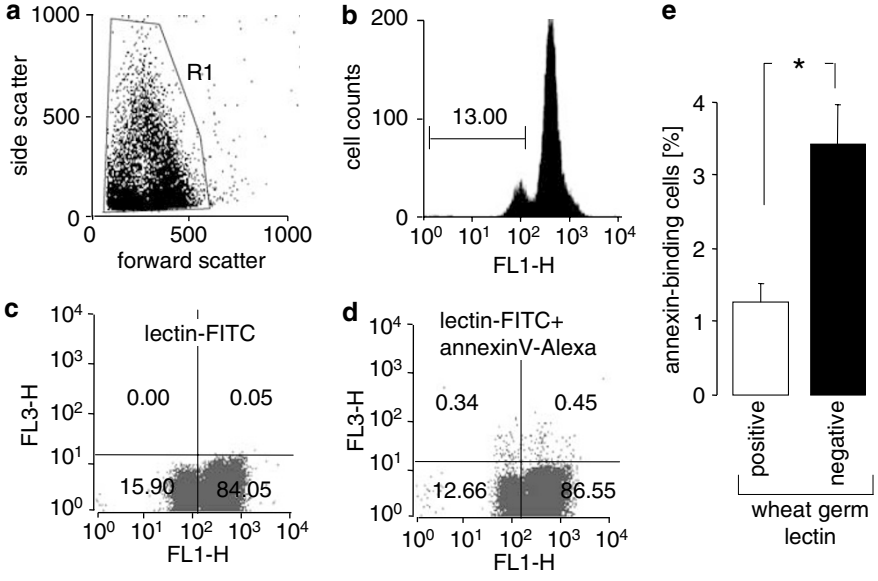

Figure 1 Percentage of phosphatidylserine-exposing erythrocytes increases with erythrocyte age. Flow cytometry of human erythrocytes double-stained with wheat germ lectin-FITC and Annexin V-Alexa. (**a**) Gated erythrocyte population in forward and sideward scatter. (**b**) Histogram of lectin-stained erythrocytes showing two cell populations with different lectin binding. (**c**, **d**) Dot plots depicting the FL-1 and the FL-3 fluorescence of (**c**) lectin-FITC-stained and (**d**) lectin-FITC/Annexin V-Alexa-double-stained erythrocytes. Numbers are the percentage of cells in the indicated plot areas. (**e**) Mean percentage of annexin-positive cells ($\pm$S.E.; $n=8$) of low lectin- (negative) and high lectin- (positive) binding erythrocytes. *$P\leqslant0.05$ two-tailed *t*-test

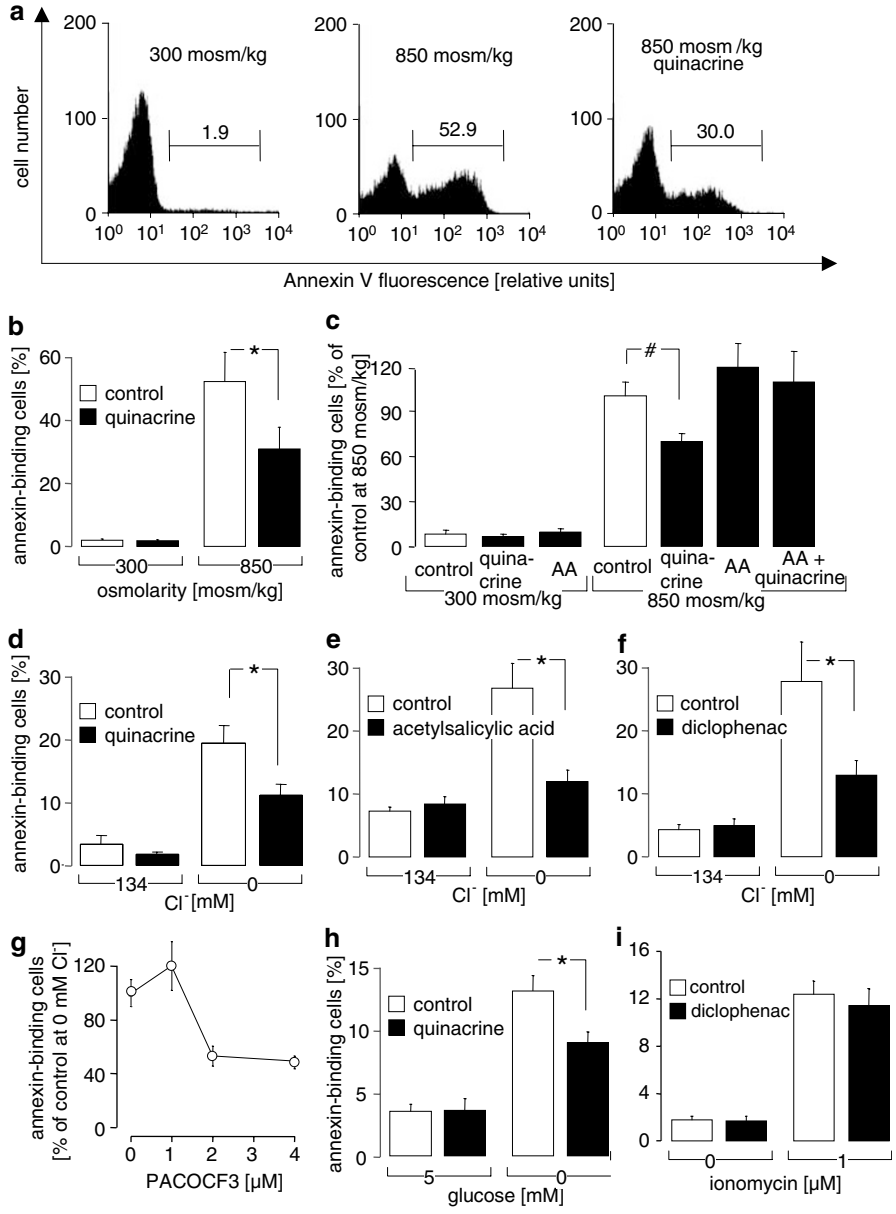

Figure 2 Dependence of erythrocyte annexin binding following osmotic shock, Cl^- removal or energy depletion on PLA_2 and COX activity. (**a**–**c**) Phosphatidylserine exposure reflected by Annexin V binding in FACS analysis of erythrocytes exposed to osmotic shock in the presence or absence of PLA_2-inhibitor quinacrine. (**a**) Representative histograms showing annexin V fluorescence of human erythrocytes incubated for 6 h in the absence (left and middle) or presence (right) of quinacrine (25 μM) in either isotonic NaCl Ringer (300 mOsm; left) or in NaCl Ringer supplemented with 550 mM sucrose (850 mOsm; middle and right). (**b**) Number of annexin-binding erythrocytes after 6-h incubation in isotonic (300 mOsm) or hypertonic (850 mOsm) NaCl Ringer solution in the absence (open bars) or presence (closed bars) of quinacrine (25 μM). The percentages of annexin-binding cells (as given by the numbers in (**a**)) were defined by their fluorescence intensity within the intensity window indicated by the bar. (**c**) Annexin-binding cells in % of control at 850 mOsm after 6 h incubation in isotonic (300 mOsm) or hypertonic (850 mOsm) Ringer solution in the absence (control, open bars) or presence (closed bars) of quinacrine (25 μM), arachidonic acid (AA, 1 μM) or quinacrine (25 μM) plus arachidonic acid (AA, 1 μM). (**d**–**f**) Inhibition of Cl^- removal-induced phosphatidylserine exposure by the PLA_2 inhibitor quinacrine and the COX inhibitors acetylsalicylic acid and diclophenac. Given are the numbers of annexin-binding erythrocytes after 48 h incubation in NaCl Ringer (134 mM Cl^-) or in Na-gluconate solution (0 mM Cl^-) in the absence (open bars) or presence (closed bars) of quinacrine (25 μM; **d**), acetylsalicylic acid (50 μM; **e**), or diclophenac (10 μM; **f**). Data in (**b**–**f**) are means $\pm$ S.E.M.; $n = 4$–10; controls were supplemented with the appropriate concentration of drug vehicle. (**g**) Effect of increasing concentrations of PACOCF3, an inhibitor of the Ca^{2+}-independent PLA_2, on Cl^- removal (48 h)-triggered annexin binding. Under PACOCF3-free control conditions 35.8 $\pm$ 7.3% of the Cl^--depleted erythrocytes bound annexin (data are means $\pm$ S.E.M.; $n = 4$). (**h**, **i**) Effect of quinacrine (25 μM) on erythrocyte annexin binding following energy depletion (0 mM glucose for 24 h; **h**) or stimulation with the Ca^{2+} ionophore ionomycin (1 μM for 1 h; **i**). Data in (**h**, **i**) are means $\pm$ S.E.M.; $n = 5$–8. $^*P \leqslant 0.05$ two-tailed *t*-test. $^{\#}P \leqslant 0.05$ ANOVA)

extracellular Ca^{2+} (Figure 3e) but blunted by 25 μM quinacrine (Figure 3f). In summary, these experiments strongly suggest triggering of Ca^{2+}-independent PGE_2 synthesis by hyperosmotic shock. PGE_2 synthesis most probably does not occur secondary to cation channel activation and channel-mediated increase in cytosolic free Ca^{2+}.

PGE_2 but not thromboxane B_2 (50 μM each) significantly stimulated the annexin binding of erythrocytes within 24 h of

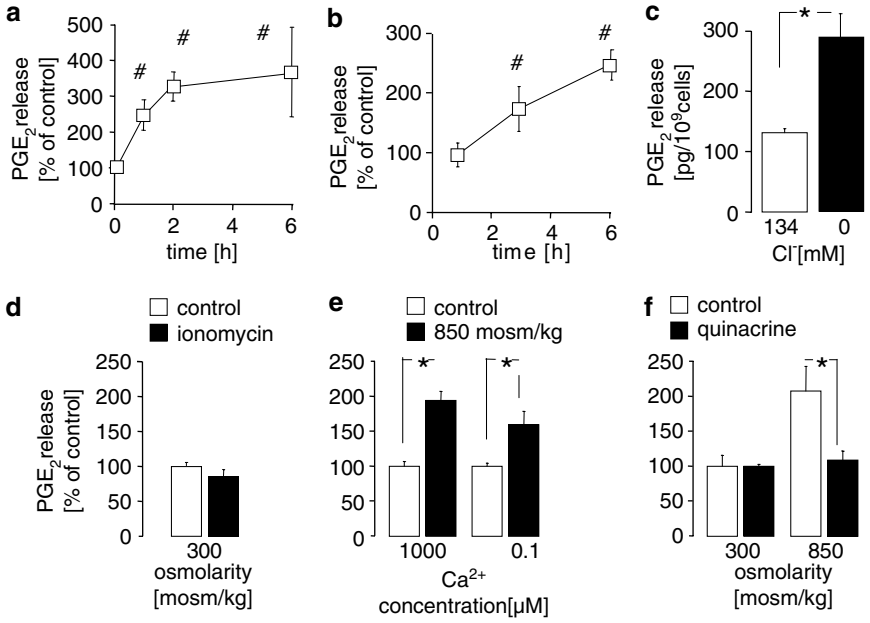

Figure 3 Formation of PGE_2. (**a**, **b**) Time-dependent stimulation of PGE_2 release by hyperosmotic shock (**a**) and extracellular Cl^--removal (**b**). Shown is the PGE_2 accumulation in the supernatant during incubation of human erythrocytes in hyperosmotic (850 mOsm; **a**) and Cl^--free medium (**b**), respectively, as determined by competitive immunoassay. Data are means ± S.E.M.; $n = 3$–5 and given as % of the controls. For controls, erythrocytes were incubated for the respective time periods in normal NaCl Ringer medium; # indicates significant difference from the respective control values ($P \leqslant 0.05$, ANOVA). (**c**) PGE_2 release during 6 h of incubation in normal NaCl Ringer (134 mM Cl^-) or Cl^--free medium (0 mM Cl^-). Data are means ± S.E.M.; $n = 3$ and given as pg/10^9 cells. *$P \leqslant 0.05$, two-tailed *t*-test). (**d**) PGE_2 release of erythrocytes incubated in isotonic Ringer solution in the absence (open bar) or presence of the Ca^{2+} ionophore ionomycin (1 μM for 1h; closed bar). (**e**) Hyperosmotic shock (1 h)-stimulated PGE_2 release in Ringer solution containing low (0.1 μM) or normal (1000 μM) free Ca^{2+} concentration. (**f**) Hyperosmotic shock (1 h)-stimulated PGE_2 release in the absence (open bars) or presence of quinacrine (25 μM; closed bars). Data in (**d**–**f**) are means ± S.E.M.; $n = 3$–5 and given as % of the controls. *$P \leqslant 0.05$, two-tailed *t*-test

incubation in isotonic NaCl Ringer solution (Figure 4a, left and middle and Figure 4b). The effect of 50 μM PGE_2 on annexin binding was abrogated in the nominal absence of extracellular Ca^{2+} (Figure 4a, right and Figure 4b). Figure 4c depicts the concentration-dependent effect of PGE_2 and thromboxane B_2 on erythrocyte annexin binding. Concentrations of PGE_2 in the range of 20–50 μM were required to stimulate annexin binding, whereas nanomolar PGE_2 concentrations did not lead to significant increases of annexin binding (data not shown).

PGE_2 (50 μM)-stimulated phosphatidylserine exposure was paralleled by proteolytic cleavage of ankyrin R as demonstrated by immunoblot (Figure 4d). Ionomycin (1 μM for 1 h) induced similar ankyrin R degradation (Figure 4e), suggesting involvement of a Ca^{2+}-activated protease in the effector phase of programmed erythrocyte death. Accordingly, ionomycin (1 μM for 1 h) or PGE_2 (50 μM for 12 h) stimulated in erythrocytes the cleavage of the latent calpain protein (p80) into its proteolytic active forms (p78 and p76) as demonstrated by immunoblotting (Figure 5a). Moreover, a mixture of calpain inhibitors I and II (177 and 70 μM, respectively) attenuated the PGE_2-induced proteolytic degradation of ankyrin R (Figure 5b; second and third lanes). In sharp contrast, calpain inhibitors I and II at the same concentrations had no effect on PGE_2 (50 μM for 24 h)-stimulated annexin binding (Figure 5c).

The effect of PGE_2 (50 μM) on annexin binding was further accompanied by sustained erythrocyte shrinkage, as evident from a decrease of forward scatter in FACS analysis. PGE_2 but not thromboxane B_2 (50 μM each) significantly decreased the forward scatter upon 24 h of incubation in isotonic NaCl Ringer (Figure 6a, left and middle, and Figure 6b). Similar to the effect of PGE_2 on annexin binding, the effect of PGE_2 on forward scatter was abolished in nominally Ca^{2+}-free Ringer solution. Figure 6c illustrates the effect of different PGE_2 and thromboxane B_2 concentrations on the erythrocyte forward scatter.

FACS analysis in erythrocytes loaded with the Ca^{2+}-sensitive Fluo-3 fluorescence dye revealed that PGE_2 applied in isotonic Ringer solution significantly increased the intracellular Ca^{2+} concentration. Subnanomolar PGE_2 concentrations rapidly enhanced intracellular Ca^{2+} activity in some 4% of the erythrocytes (Figure 7a, b). At higher concentrations of PGE_2 (50 μM) Ca^{2+} activity was increased in almost half of the cells (Figure 7c, middle panel). The cytosolic Ca^{2+} concentration of erythrocytes stimulated with 50 μM PGE_2 continued to increase throughout the 4 h of recording time (Figure 7e), suggesting a sustained Ca^{2+} increase by PGE_2. The Ca^{2+} ionophore ionomycin (1 μM), which was used as a positive control, similarly increased Fluo-3 fluorescence intensity of erythrocytes (Figure 7d).

To identify the pathway of PGE_2-stimulated Ca^{2+} influx, erythrocyte whole-cell currents were recorded during stimulation with PGE_2. The membrane conductance of human erythrocytes in NaCl Ringer solution and the absence of exogenous PGE_2 (Figure 8a, b, left tracings and Figure 8c, open symbols) amounted to some 100 pS (Figure 8d, white

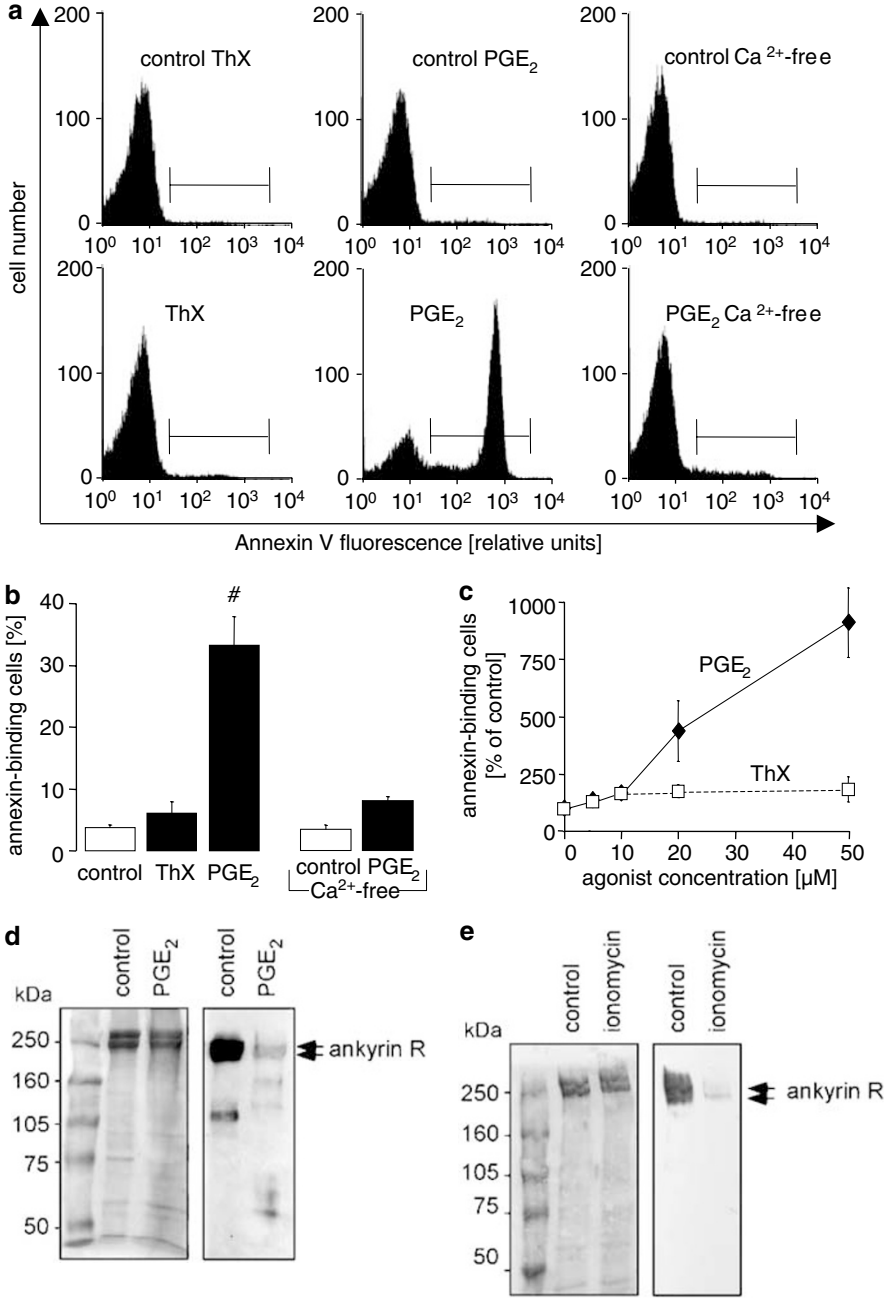

Figure 4 Effect of PGE_2 on phosphatidylserine exposure and ankyrin R degradation. (**a**) Representative FACS histograms depicting the annexin V fluorescence of erythrocytes (as a measure of phosphatidylserine exposure) incubated for 24 h in vehicle-containing NaCl Ringer (control; upper panels) or in NaCl Ringer solution containing thromboxane B_2 (ThX; 50 μM; lower left) or PGE_2 (50 μM, lower middle and right). Experiments were performed either in normal Ca^{2+}-containing NaCl Ringer (left and middle) or in EGTA-buffered Ca^{2+}-free NaCl Ringer (right). (**b**) Mean percentage of annexin V-binding erythrocytes ($\pm$S.E.M.; $n = 6$–14) stimulated as in (**a**) in the presence or nominal absence (Ca^{2+}-free) of extracellular Ca^{2+} with vehicle alone (control), thromboxane (ThX; 50 μM), or PGE_2 (50 μM) (# indicates significant difference from controls; $P \leqslant 0.05$; ANOVA). (**c**) Concentration dependence of the PGE_2 (closed diamonds) and thromboxane B_2 (ThX, open squares) effect on erythrocyte annexin binding after 24 h incubation in normal Ca^{2+}-containing NaCl Ringer. Data are means $\pm$S.E.M. ($n = 9$–13) and given as % of the controls. For controls, erythrocytes were incubated for 24 h in vehicle- and Ca^{2+}-containing NaCl Ringer. (**d**, **e**) Nonspecific protein (Ponceau red, left) and specific ankyrin R immunostaining (right) of Western blots from human erythrocyte membranes. Erythrocytes were either incubated at 37°C for 12 h in the presence or absence of PGE_2 (50 μM; **d**) or for 1 h in the presence or absence of the Ca^{2+} ionophore ionomycin (1 μM; **e**)

bars). This value was in the range of the expected leak conductance generated by a 10 MΩ seal resistance indicating no or very low basal ion channel activity under the chosen experimental condition. Bath application of PGE_2 (0.1 and 50 μM; Figure 8a, b, second tracings) but not of vehicle alone increased within 5 min of incubation a slightly outwardly rectifying whole-cell current (Figure 8c, closed circles) accompanied by an increase of whole-cell conductance to

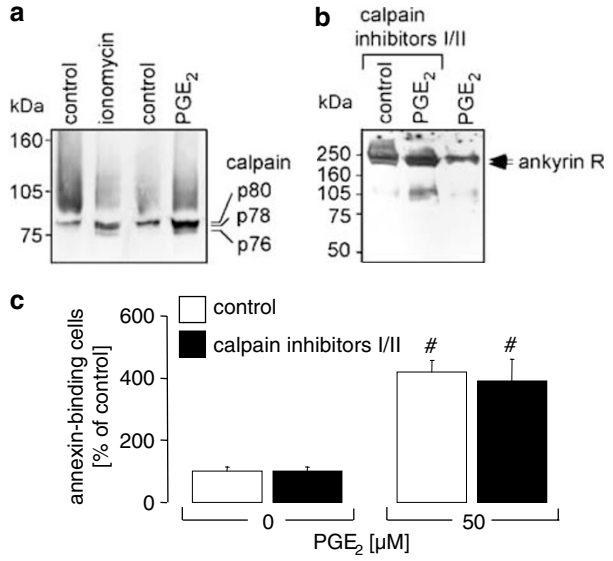

Figure 5 Calpain inhibitors attenuate PGE_2-stimulated ankyrin R degradation but not PGE_2-stimulated phosphatidylserine exposure. (**a**) Immunoblot showing calpain-specific immunoreactive protein bands p80, p78, and p76 of erythrocytes incubated in NaCl Ringer solution in the absence or presence of ionomycin (1 μM for 1 h; first and second lanes, respectively) or in the absence or presence of PGE_2 (50 μM for 12 h, third and fourth lanes, respectively). Both ionomycin and PGE_2 stimulated the proteolytic cleavage of the latent form of calpain (p80) into its active forms (p78 and p76). (**b**) Ankyrin R-specific immunoblot of control (vehicle for 12 h; first lane) or PGE_2 (50 μM for 12 h)-stimulated erythrocytes which were pre- (30 min) and coincubated (12 h) with a mixture of calpain inhibitors I and II (177 and 70 μM, respectively; second lane) or vehicle alone (third lane). (**c**) Annexin binding showing phosphatidylserine exposure of PGE_2- (50 μM for 24 h; right columns) or vehicle-incubated (24 h; left columns) erythrocytes. Stimulation was performed either in the presence (black columns) or absence (white columns) of calpain inhibitors I and II (177 and 70 μM, respectively; 30 min pre- and 24 h coincubation). Data are means $\pm$ S.E.M.; $n=7$; # indicates significant difference from the respective controls; $P \leqslant 0.05$; ANOVA)

about 400 pS (as calculated for the outward current; Figure 8d, closed bars). This current exhibited a reversal potential close to 0 mV when recorded with K-gluconate/KCl pipette and NaCl Ringer bath solution (Figure 8c, closed circles). Replacement of Na^+ in the bath by the impermeant cation *N*-methyl-D-glucamine $(NMDG)^+$ shifted the reversal potential to about -60 mV, paralleling the change of the equilibrium potential for the permeant cations (Figure 8c, closed triangles), which indicates cation selectivity of the PGE_2-stimulated current. The cation channel blocker ethylisopropylamiloride (EIPA; 10 μM) reversibly inhibited the PGE_2-stimulated current (Figure 8b, d). Taken together, these data demonstrate PGE_2-induced activation of EIPA-sensitive nonselective cation channels in human erythrocytes.

To further test whether the reported activation of nonselective cation channels by removal of extracellular Cl^- might also be mediated by PGE_2, erythrocyte whole-cell currents were recorded in Na-gluconate bath solution in the presence and absence of diclophenac. As shown in Figure 8e–h, incubation of erythrocytes in Na-gluconate solution in the presence of diclophenac (10 μM) did not induce any increase in whole-cell currents (Figure 8e, outer left and middle left, and Figure 8f, open circles and closed triangles), while subsequent wash-out of diclophenac by Na-gluconate solution reversibly increased the whole-cell currents (Figure 8e, middle right and outer right). The current induced by incubation in diclophenac-free Na-gluconate solution reversed at 0 mV (K-gluconate/KCl-pipette solution; Figure 8f, open triangles), indicating its nondiscriminating cation selectivity. Figure 8g summarizes the whole-cell conductances (as calculated for the outward current) in NaCl Ringer, in Na-gluconate bath solution in the presence or absence of diclophenac (10 μM) and again in NaCl as obtained in paired experiments. Diclophenac significantly blunted the increase in whole-cell conductance of erythrocytes following removal of extracellular Cl^- (Figure 8h), indicating the involvement of cyclooxygenase in cation channel activation.

Discussion

The present study confirms that osmotic shock, which triggers apoptotic death in a wide variety of nucleated cells,[8,28–30] is a similarly powerful stimulus of erythrocyte apoptosis. Even though erythrocytes lack nuclei and mitochondria, they are capable of undergoing some of the morphological features of apoptosis, such as external exposure of phosphatidylserine, membrane blebbing and cell shrinkage.[4] All those events are triggered by increase of cytosolic calcium activity,[2,3] while erythrocytes are resistant to serum deprivation and staurosporine, known triggers of apoptosis in nucleated cells.[4]

As shown in previous studies,[5–7] erythrocyte cell shrinkage activates Ca^{2+} entry through EIPA-sensitive, cell volume-regulated cation channels characterized earlier.[20,21,31] Similar to osmotic shock, oxidative stress leads to marked erythrocyte shrinkage, an effect probably resulting from activation of the Ca^{2+}-sensitive K^+ channel in the erythrocyte cell membrane, which leads to hyperpolarization of the cell membrane and subsequent erythrocyte loss of KCl.[17,18,32]

Most importantly, several observations reported here indicate that the signalling of channel activation involves PGE_2, which is produced from membrane phospholipids by the sequential action of Ca^{2+}-independent PLA_2, cyclooxygenase and PGE-synthase. It is demonstrated that (i) cell shrinkage and Cl^- removal trigger the formation of PGE_2, an effect abrogated by the PLA_2 inhibitor quinacrine, (ii) PGE_2 stimulates the cation channels, and (iii) inhibition of either PLA_2 or cyclooxygenase blunts the phosphatidylserine exposure following osmotic shock, external Cl^- removal or energy depletion. The observations thus do suggest the following sequence of events (Figure 9): cell shrinkage or extracellular Cl^- removal activates the cyclooxygenase, PGE_2 is formed and activates the cation channel, entry of Ca^{2+} through the channel stimulates the scramblase, which then triggers the phosphatidylserine exposure. Elevated cytosolic free Ca^{2+} concentrations also activate μ-calpain, which degrades components of the cytoskeleton, for example, ankyrin R, leading to membrane blebbing. However, stimulation of calpain and scramblase are not functionally linked as PGE_2-induced phosphatidylserine exposure is not inhibited by calpain inhibitors I/II. The latter result is in accordance with a previous study demonstrating that ionomycin-induced

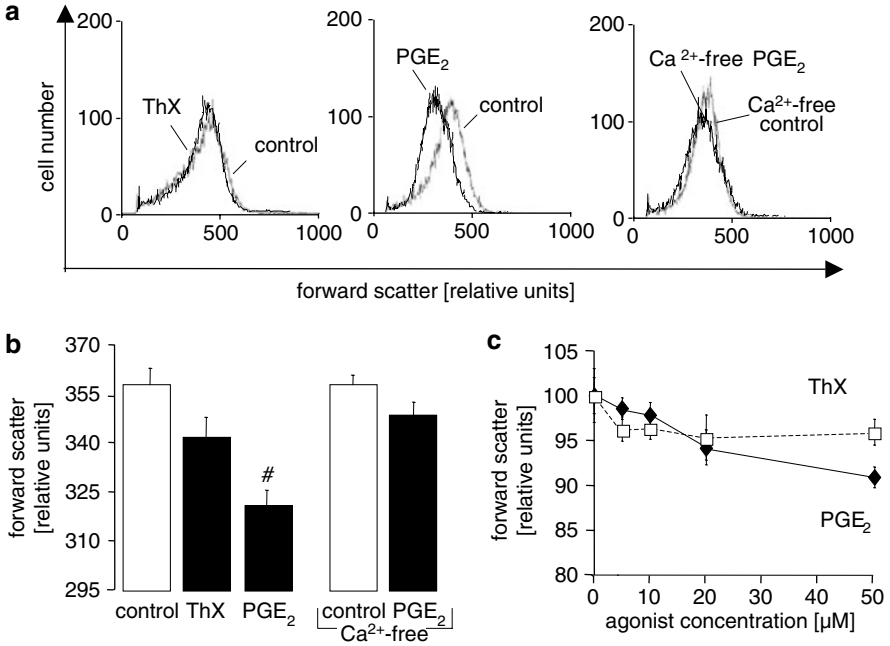

Figure 6 PGE_2-stimulated cell shrinkage. (**a**) Representative FACS histograms depicting the forward scatter of erythrocytes (as a measure of erythrocyte volume) incubated for 24 h in NaCl Ringer (control) or in NaCl Ringer solution containing thromboxane B_2 (ThX; 50 μM; left) or PGE_2 (50 μM, middle and right). Experiments were performed either in normal Ca^{2+}-containing NaCl Ringer (left and middle) or in EGTA-buffered Ca^{2+}-free NaCl Ringer (right). (**b**) Mean forward scatter ($\pm$S.E.M.; $n = 6$–9) of erythrocytes stimulated as in (**a**) in the presence or nominal absence (Ca^{2+}-free) of extracellular Ca^{2+} with vehicle alone (control), thromboxane B_2 (ThX; 50 μM), or PGE_2 (50 μM) (# indicates significant difference from controls; $P \leqslant 0.05$; ANOVA). (**c**) Concentration dependence of the PGE_2 (closed diamonds) and thromboxane B_2 (ThX, open squares) effect on erythrocyte forward scatter after 24 h incubation in normal Ca^{2+}-containing NaCl Ringer. Data are means $\pm$ S.E.M. ($n = 6$–9) and given as % of the controls. For controls, erythrocytes were incubated for 24 h in vehicle- and Ca^{2+}-containing NaCl Ringer

annexin binding was not reduced by calpain inhibitors I/II.[2] Release of PGE_2 upon decrease of extracellular Cl^- is not a property confined to human erythrocytes. Macula densa cells have been demonstrated to similarly release PGE_2 upon Cl^- removal. In these cells, low Cl^- concentrations induced COX protein expression through MAP kinases activation.[33]

In a former study, it has been shown that mechanically stressed adult human red blood cells produce PGE_2.[34] Furthermore, evidence was presented earlier for PGE_2-induced activation of a nonselective cation channel,[22] for PGE_2 stimulated increase in cytosolic free Ca^{2+} concentration,[23] and PGE_2-induced release of K^+ from erythrocytes, which was blunted by inhibitors of Ca^{2+}-dependent K^+ channels.[25] As PGE_2 activates the Ca^{2+}-permeable cation channel, it increases cytosolic Ca^{2+}, thus leading to secondary activation of the Ca^{2+}-dependent K^+ channels.[35,36] The subsequent cellular release of K^+ and Cl^- together with osmotically obliged water then leads to cell shrinkage.[25] Beyond that the cellular loss of K^+ participates in the triggering of erythrocyte scramblase.[19] Along those lines, apoptotic death of nucleated cells has similarly been shown to be fostered by cellular loss of K^+.[37–43]

In the present study, hyperosmotic shock, removal of extracellular Cl^-, and glucose depletion stimulated average erythrocyte phosphatidylserine exposures of about 50, 25, and 12% of the cells, respectively. In addition, the percentage of cells responding to a certain stress stimulus varied between individual experiments. Moreover, in accordance with a previous study,[25] we could demonstrate that a small but significant part of the erythrocytes (4%) responded to subnanomolar concentrations of PGE_2 with an increase in cytosolic free Ca^{2+} concentration (Figure 7a, b) and cell shrinkage. High PGE_2 concentrations (50 μM), however, stimulated an increase in cytosolic Ca^{2+} concentrations and phosphatidylserine exposure in about 50 and 35% of the erythrocytes, respectively. This suggests that only an erythrocyte subpopulation is highly susceptible to PGE_2. Thus, whether or not erythrocytes respond to the various stress factors or to PGE_2 and enter programmed cell death might be dependent on further parameters (cytosolic ATP concentration, redox state, cell volume). These parameters might differ between individual erythrocytes from the same donor and between individual cell preparations from different donors. The observation of the present and a previous study[26] that erythrocyte phosphatidylserine exposure increases with the age-dependent desialylation of the membrane glycoconjugates further illustrates such differences.

PGE_2 concentrations in the range of 20 μM were required in the present study to stimulate erythrocyte phosphatidylserine exposure, indicating that Ca^{2+} influx and cell shrinkage induced by nanomolar PGE_2 concentrations are transient and do not result in erythrocyte death. Nevertheless, the fact that COX and PLA_2 inhibitors significantly blunt the stress-induced cation channel activation and phosphatidylserine exposure clearly shows involvement of the PGE_2 signalling in erythrocyte death upstream from cation channel activation.

Formation of PGE_2 by stressed erythrocytes could therefore well participate in the limitation of erythrocyte survival.

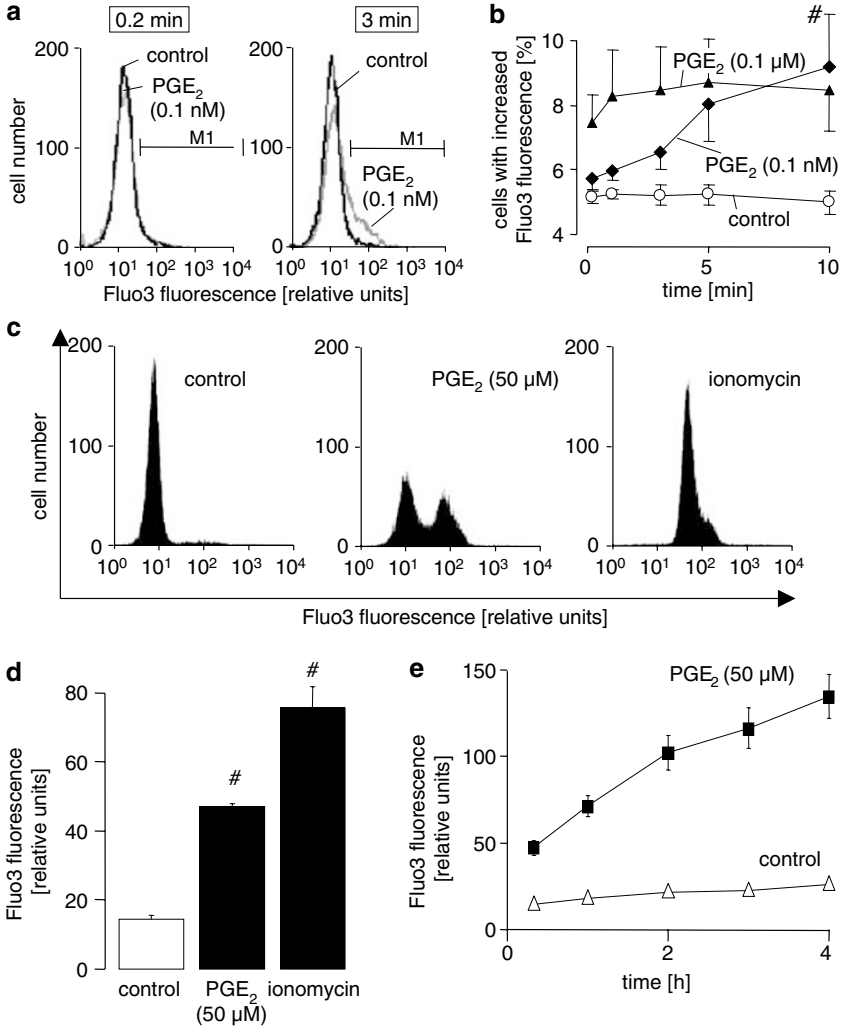

Figure 7 PGE_2 stimulated increase in erythrocyte free Ca^{2+} concentration. (**a**) Representative FACS histograms showing the Ca^{2+}-sensitive fluorescence of Fluo-3-loaded erythrocytes incubated for 0.2 min (left) or 3 min (right) in NaCl Ringer solution containing vehicle (control) or 0.1 nM PGE_2. Erythrocytes gated in M1 were considered to exhibit elevated Fluo-3 fluorescence intensities. (**b**) Time-dependent increase in percentage of erythrocytes with elevated Fluo-3 fluorescence during stimulation with 0 nM (control; open circles), 0.1 nM (closed diamonds) and 0.1 μM PGE_2 (closed triangles). Cells with elevated Fluo-3 fluorescence were defined as in (**a**). Data are means $\pm$ S.E.M. ($n = 9$–12); # indicates significant difference ($P \leqslant 0.05$; ANOVA) from controls. (**c**) Representative FACS histograms showing the Ca^{2+}-sensitive fluorescence of Fluo-3-loaded erythrocytes incubated for 20 min either in NaCl Ringer solution (left), in NaCl Ringer containing PGE_2 (50 μM; middle), or in NaCl Ringer containing the Ca^{2+} ionophore ionomycin (1 μM; right). (**d**) Mean fluorescence ($\pm$ S.E.M.; $n = 6$–10) of erythrocytes incubated as in (**c**) for 20 min in the absence (control) or presence of PGE_2 (50 μM) or ionomycin (1 μM). # indicates significant difference ($P \leqslant 0.05$; ANOVA) from controls. (**e**) Time course of Fluo-3 fluorescence in erythrocytes incubated in NaCl Ringer solution in the absence (open triangles) or presence of PGE_2 (50 μM; closed squares). Data are means $\pm$ S.E.M. ($n = 6$)

Figure 8 PGE_2-induced activation of an EIPA-sensitive nonselective cation conductance. (**a**, **b**) Original whole-cell currents recorded from a human erythrocyte with K-gluconate/KCl pipette and NaCl bath solution before (outer left) and after bath application of 0.1 μM (**a**) and 50 μM PGE_2 (**b**). The PGE_2-stimulated cell in (**b**) was recorded either in the absence (middle left and outer right) or presence (middle right) of EIPA (10 μM) in the bath solution. (**c**) Mean current–voltage relationships ($\pm$ S.E.M.) of human erythrocytes recorded as in (**b**) in paired experiments before (open circles) and after (closed circles) stimulation with PGE_2 (50 μM for 4 ± 1 min; $n = 8$). The PGE_2-stimulated cells were further recorded with NMDG-Cl bath solution ($n = 3$; closed triangles). (**d**) Mean whole-cell conductance ($\pm$ S.E.M.) of nontreated erythrocytes (open bars) or erythrocytes incubated either with vehicle alone (0.5% ethanol; first closed bar), or with PGE_2 (50 μM; second closed bar), or PGE_2 (50 μM) together with EIPA (10 μM; third closed bar). Currents were recorded as in (**b**) and conductances were calculated by linear regression for outward and inward currents beween -100 and 0 mV and between $+40$ and $+80$ mV voltage, respectively (*n* indicates number of experiments; $^{**}P \leqslant 0.01$, ANOVA). (**e**) Original whole-cell currents recorded from a human erythrocyte in NaCl bath solution (outer left; K-gluconate/KCl pipette solution), upon 5 min superfusion with Na-gluconate bath solution supplemented with diclophenac (10 μM; middle left), upon further 5 min superfusion with inhibitor-free Na-gluconate bath solution (middle right), and finally again in NaCl bath solution (outer right). (**f**) Mean current–voltage relationships ($\pm$ S.E.M.; $n = 7$) of human erythrocytes superfused as in (**e**) in paired experiments first with NaCl bath solution (open circles), then with Na-gluconate solution supplemented with 10 μM diclophenac (for 4.8 ± 0.2 min; closed triangles) and finally with Na-gluconate solution alone (for 3.4 ± 0.4 min; open triangles). (**g**) Mean whole-cell outward conductance ($\pm$ S.E.M.; $n = 7$) of erythrocytes consecutively recorded as in (**e**, **f**) with NaCl (first bar), with Na-gluconate/diclophenac (10 μM; second bar) and with Na-gluconate (third bar) or again with NaCl (fourth bar). (**h**) Mean conductance increase ($\pm$ S.E.M.; $n = 7$) induced by removal of extracellular Cl^- in the presence (closed bar) or absence (open bar) of diclophenac (10 μM; data calculated from (**g**); $^{**}P \leqslant 0.01$ two-tailed *t*-test)

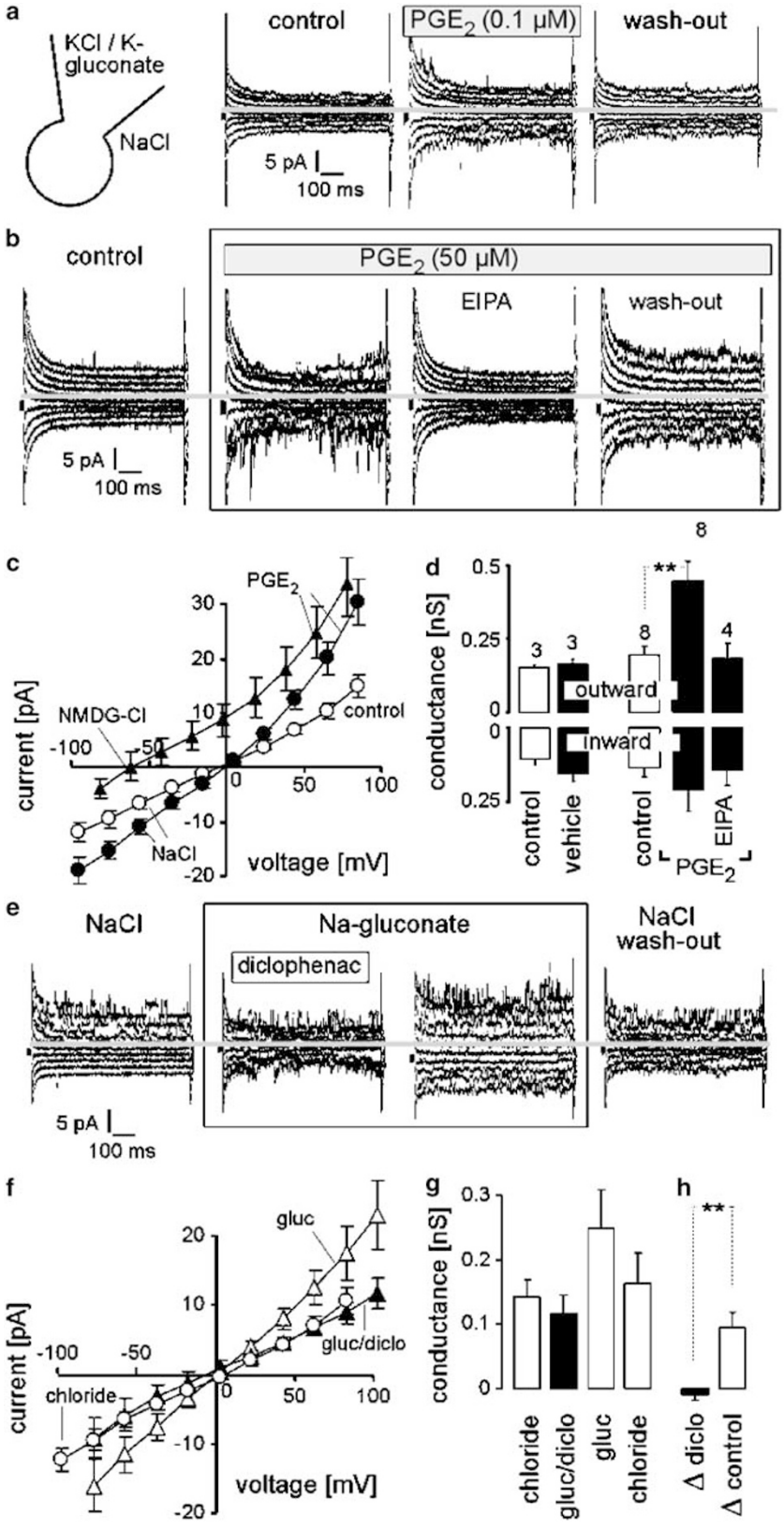
a
KCl / K-gluconate
NaCl
control
PGE2 (0.1 µM)
wash-out
5 pA
100 ms
b
control
PGE2 (50 µM)
EIPA
wash-out
5 pA
100 ms
8
c
PGE2
control
NMDG-Cl
NaCl
current [pA]
voltage [mV]
d
conductance [nS]
outward
inward
control
vehicle
control
EIPA
PGE2
e
NaCl
Na-gluconate
diclophenac
NaCl wash-out
5 pA
100 ms
f
gluc
gluc/diclo
chloride
current [pA]
voltage [mV]
g
conductance [nS]
chloride
gluc/diclo
gluc
chloride
h
Δ diclo
Δ control

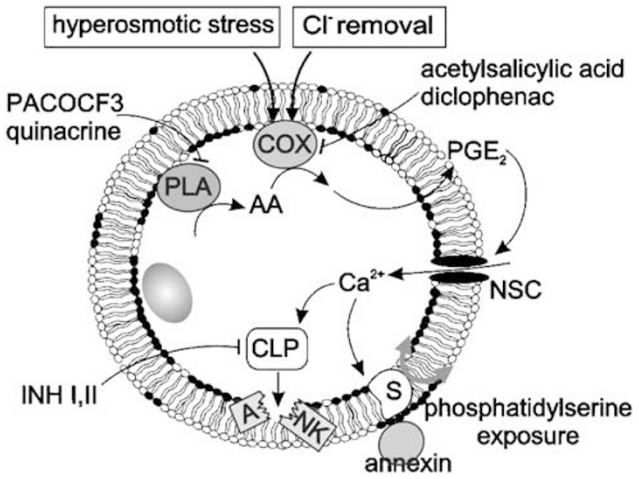

Figure 9 Role of PGE_2 in programmed erythrocyte death after hyperosmotic shock and chloride removal. Hypothetical model of the downstream signalling events stimulating phosphatidylserine exposure and ankyrin R degradation in human erythrocytes subjected to hyperosmotic stress or extracellular Cl^- removal (AA: arachidonic acid; ANK: ankyrin-R; CLP: calpain; COX: cyclooxygenase; INH I,II: calpain inhibitors I,II; NSC: nonselective cation channel; PACOCF3: palmitoyltrifluoromethyl ketone; PGE_2: prostaglandin E_2; PLA: phospholipase A_2; S: scramblase)

The phosphatidylserine exposure at the cell surface is thought to stimulate the uptake by macrophages.[14,44] Moreover, the present study demonstrated Ca^{2+}-ionophore and PGE_2-triggered proteolysis of ankyrin R (band 2.1), an effect paralleled by the activation of μ-calpain and inhibited by calpain inhibitors I/II. These data are consistent with PGE_2-induced ankyrin R proteolysis by the Ca^{2+}-dependent neutral endopeptidase calpain, which has been shown to degrade ankyrin R (about 215 kDa) *in vitro* to several cleavage products.[45,46] Thus, PGE_2 may lead to calpain-mediated disruption of the cytoskeleton followed by shedding of microvesicles and decrease of erythrocyte cell mass, which further facilitates phagocytosis by macrophages. Caspases comprise a family of cysteine endopeptidases expressed in erythrocytes.[47,48] However, the role of caspases during stress-induced programmed erythrocyte death seems to be more complex. Oxidative stress[47] and erythrocyte aging[48] obviously lead to stimulation of caspase-3 and degradation of target proteins, for example, erythrocyte anion exchanger 1 (band 3), while caspases are not activated after hyperosmotic shrinkage[7] or ionomycin treatment.[2]

Thus, to the extent that calcium activates the enzymes responsible for the breakdown of membrane phosphatidylserine asymmetry and degradation of the cytoskeleton, an increase of cytosolic Ca^{2+} activity is expected to trigger the clearance of the affected erythrocytes.[4] This may be also important for erythrocyte aging, which is paralleled by an increase of cytosolic Ca^{2+} activity.[44,49] Moreover, oxidative stress or defects of antioxidative defence[50] clearly enhance Ca^{2+} entry via the cation channels. This in turn leads to higher intracellular Ca^{2+} concentrations and thus accelerates erythrocyte 'apoptosis' and clearance.

During passage of the renal medulla, erythrocytes are exposed to excessive osmolarities sufficient to activate the cation channel. Normally, the exposure is too short, though, to trigger apoptosis. Nevertheless, it is noteworthy that during acute renal failure erythrocytes may be trapped in renal medulla.[51,52] The subsequent erythrocyte 'apoptosis' may then contribute to the derangement of microcirculation. Beyond that any erythrocyte disorder facilitating erythrocyte shrinkage, such as sickle cell disease,[28,53] thalassemia[54] or iron deficiency[55] could, to the extent as it leads to activation of the cell volume regulatory cation channels, trigger premature 'apoptosis' and thus accelerate erythrocyte death.[56]

Erythrocyte phosphatidylserine exposure may not only be regulated by PGE_2 formed by stressed erythrocytes but also may be triggered by PGE_2 from other sources. Indeed, we could show here that extracellularly added PGE_2 induces cell shrinkage, Ca^{2+} entry and phosphatidylserine exposure of nonstressed erythrocytes. PGE_2 released from platelets may thus trigger erythrocyte phosphatidylserine exposure, which may participate in the mechanism of thrombosis and hemostasis.[25] Several lines of evidence indeed point to a role of erythrocytes in the regulation of hemostasis.[57–60]

Beyond that, PGE_2 is a highly active mediator in inflammation, chemotactic processes, and cell damage (for review see Laufer[61]). PGE_2-dependent regulation of cation channels may also play a role in nucleated cells which similarly express cell volume regulatory cation channels.[62–67] As increase of cytosolic Ca^{2+} could similarly induce apoptotic cell death in nucleated cells,[1,68] activation of the volume-regulated cation channels might participate in the triggering of apoptosis in nucleated cells exposed to osmotic shock.[8,29,30,69,70] However, it must be pointed out that the mechanisms triggering phosphatidylserine exposure in erythrocytes may be distinct from those inducing apoptosis of nucleated cells. Nevertheless, phosphatidylserine exposure of erythrocytes serves the same function as apoptosis of nucleated cells, that is, the clearance of defective and potentially harmful cells.

Materials and Methods

Solutions

Erythrocytes were drawn from healthy volunteers and used either without purification or after separation by centrifugation for 25 min; 2000 × *g* over Ficoll (Biochrom KG, Berlin, Germany). Experiments with nonpurified or experiments with Ficoll-separated erythrocytes yielded the same results (data not shown). Experiments were performed at 37°C in Ringer solution containing (in mM) 125 NaCl, 5 KCl, 1 $MgSO_4$, 32 *N*-2-hydroxyethylpiperazine-*N*-2-ethanesulfonic acid (HEPES)/NaOH, 5 glucose, 1 $CaCl_2$, pH 7.4. For the nominally calcium-free solution, $CaCl_2$ was replaced by 1 mM ethylene glycol-bis(β-aminoethyl ether)-*N,N,N′,N′*-tetraacetic acid (EGTA). For energy depletion, glucose (5 mM) was omitted from the NaCl Ringer solution. Osmolarity was increased to 850 mOsm by adding sucrose to the NaCl Ringer solution. Cl^--free solutions were composed of (in mM) 125 Na-D-gluconate, 5 K-D-gluconate, 1 $MgSO_4$, 32 HEPES/NaOH, 5 glucose, 1 Ca-gluconate$_2$, pH 7.4. Where indicated, the Ca^{2+} ionophore ionomycin (1 μM), the cation channel inhibitor EIPA (10 μM), PLA_2 inhibitors quinacrine (25 μM), PACOCF3 (1–4 μM) or arachidonyltrifluoromethyl ketone (AACOCF3; 8 μM), COX inhibitors acetylsalicylic acid (50 μM) or diclophenac (10 μM), prostaglandin PGE_2 (0.1 nM–50 μM), calpain inhibitor I (*N*-acetyl-L-leucyl-L-leucyl-L-norleucinal; 177 μM) and calpain inhibitor II (*N*-acetyl-L-leucyl-L-leucyl-L-methional; 70 μM), or

arachidonic acid (1 μM) and thromboxane B_2 (5–50 μM) were added. The substances were dissolved in final concentrations of 0.1% dimethyl sulfoxide (DMSO) (ionomycin, EIPA, quinacrine, acetylsalicylic acid, diclophenac, PACOCF3, AACOCF3) or of 0.5% ethanol (PGE_2, thromboxane B_2, calpain inhibitors I and II). Ionomycin, arachidonic acid, EIPA, quinacrine, acetylsalicylic acid, diclophenac, calpain inhibitor I, calpain inhibitor II, PGE_2 and thromboxane B_2 were purchased from Sigma (Taufkirchen, Germany), PACOCF3 and AACOCF3 from Merck Biosciences GmbH (Bad Soden; Germany).

Patch clamp

Patch-clamp experiments have been performed at 35°C in voltage-clamp, fast-whole-cell mode according to Hamill *et al*.[71] The cells were continuously superfused through a flow system inserted into the dish. The bath was grounded via a bridge filled with NaCl Ringer solution. Borosilicate glass pipettes (8–12 MΩ tip resistance; GC 150 TF-10, Clark Medical Instruments, Pangbourne, UK) manufactured by a microprocessor-driven DMZ puller (Zeitz, Augsburg, Germany) were used in combination with a MS314 electrical micromanipulator (MW, Märzhäuser, Wetzlar, Germany). The currents were recorded by an EPC-9 amplifier (Heka, Lambrecht, Germany) using Pulse software (Heka) and an ITC-16 Interface (Instrutech, Port Washington, NY, USA). Whole-cell currents were determined at 10 successive 700-ms square pulses from the −30 mV holding potential to potentials between −100 mV and + 80 mV. The current values were 3 kHz low-pass filtered.

A K-gluconate/KCl pipette solution (containing (in mM): 60 K-D-gluconate, 80 KCl, 1 EGTA, 1 MgCl2, 1 Mg-ATP, and 10 HEPES/KOH, pH 7.2) was used in combination with NaCl Ringer solution, NMDG-Cl solution (containing (mM): 160 mM NMDG-Cl, 10 mM HEPES/NMDG, pH 7.4) or Na- gluconate solution in the bath (containing (in mM): 125 Na-D-gluconate, 5 K-D-gluconate, 1 $MgSO_4$, 32 HEPES/NaOH, 5 glucose, 1 Ca-$gluconate_2$, pH 7.4).

The offset potentials between both electrodes were zeroed before sealing. The potentials were corrected for liquid junction potentials as estimated according to Barry and Lynch.[72] The original whole-cell current traces are depicted after 1.5 kHz low-pass filtering and currents of the individual voltage square pulses are superimposed. The applied voltages refer to the cytoplasmic face of the membrane with respect to the extracellular space. The inward currents, defined as flow of positive charge from the extracellular to the cytoplasmic membrane face, are negative currents and depicted as downward deflections of the original current traces.

FACS analysis

FACS analysis was performed essentially as described.[73] After incubation, cells were washed in annexin-binding buffer containing (in mM): 125 NaCl, 10 HEPES, pH 7.4) and 5 $CaCl_2$. Erythrocytes were stained with Annexin-Fluos (Böhringer Mannheim, Germany) at a 1 : 100 dilution. After 15 min, samples were diluted 1 : 5 and measured by flow cytometric analysis (FACS-Calibur from Becton Dickinson, Heidelberg, Germany). Cells were analyzed by forward and sideward scatter and annexin-fluorescence intensity was measured in FL-1 with an excitation wavelength of 488 nm and an emission wavelength of 530 nm.

Measurement of intracellular Ca^{2+}

Intracellular Ca^{2+} measurements were performed as described.[74] Briefly, erythrocytes were loaded with Fluo-3/AM (Calbiochem; Bad Soden, Germany) by addition of 10 μl of a Fluo-3/AM stock solution (2.0 mM in DMSO) to 10 ml erythrocyte suspension (0.16% hematocrit in Ringer). The cells were incubated at 37°C for 15 min under vigorous shaking and protection from light. An additional 10 μl of Fluo-3/AM was added, with incubation carried out for 25 min. Fluo-3/AM-loaded erythrocytes were centrifuged at 1000 × *g* for 3 min at 22°C and washed two times with Ringer solution containing 0.5% bovine serum albumin (BSA; Sigma) and once with Ringer. For flow cytometry, Fluo-3/AM-loaded erythrocytes were resuspended in 5 ml Ringer (0.32% hematocrit) containing PGE_2 (0.1 nM, 0.1 μM or 50 μM), the Ca^{2+} ionophor ionomycin (1 μM; Sigma) or vehicle alone and incubated for different time periods at 37°C. Then, Ca^{2+}-dependent fluorescence intensity was measured in fluorescence channel FL-1.

Wheat germ lectin-annexin V double staining

Human type A erythrocytes (0.2% hematocrit) were stained in 50 μl of PBS containing 5 μg/ml fluorescein isothiocyanate (FITC)-conjugated *Triticum vulgare* lectin (WGA) from wheat germ (EY Laboratories, San Mateo, CA, USA). After 10 min, 350 μl annexin-binding buffer containing (in mM) 125 NaCl, 10 HEPES (pH 7.4) and 5 $CaCl_2$ were added. Cells were pelleted at 800 × *g* for 5 min and the supernatant was discarded. Erythrocytes were then stained with 50 μl of Annexin V, Alexa Fluor® 568 conjugate (Molecular Probes, Leiden, The Netherlands) at a 1 : 50 dilution in annexin-binding buffer. After 10 min, samples were diluted 1 : 5 with annexin-binding buffer and measured by flow-cytometric analysis (FACS-Calibur from Becton Dickinson). Cells were analyzed by forward and side scatter. Lectin-FITC fluorescence intensity was measured in FL-1 with an excitation wavelength of 488 nm and an emission wavelength of 530 nm and Annexin V-Alexa Fluor® 568 fluorescence intensity was measured in FL-3 with an excitation wavelength of 488 nm and an emission wavelength of 670 nm. Gating of single erythrocytes was achieved by analysis of FSC *versus* SSC dot plots using the CellQuest™ software (see Figure 1a).

Determination of PGE_2

One billion erythrocytes were treated with 0.9 ml hypertonic NaCl Ringer solution (850 mOsm) in the absence or presence of Ca^{2+} (1 mM), hypertonic NaCl Ringer solution (850 mOsm) in the absence or presence of 25 μM quinacrine, isotonic Na-gluconate solution (0 mM Cl^-), ionomycin (1 μM) or isotonic NaCl Ringer solution (300 mOsm) as control. After incubation, cells were pelleted by centrifugation at 4°C, 450 × *g* for 5 min. The supernatant was removed and stored at −20°C. The cells were lysed by addition of 0.4 ml 10 mM HEPES (pH 7.4). The lysate was cleared by centrifugation at 4°C, 22 000 × *g* for 10 min and likewise stored at −20°C. PGE_2 concentrations in the supernatant and in the lysate were determined using the Correlate-EIA™ Prostaglandin E_2 Enzyme Immunoassay Kit from Assay Designs, Inc. (Ann Arbor, MI, USA) according to the manufacturer's instructions. Briefly, the samples were diluted 1 : 2.5 with assay buffer. Then, 100 μl sample, 50 μl alkaline phosphatase PGE_2 conjugate and 50 μl monoclonal anti-PGE_2 EIA antibody were applied to goat anti-mouse IgG microtiter plates and incubated at room temperature for 2 h. After washing, 200 μl *p*-nitrophenyl phosphate substrate solution was added and incubated at room temperature for 45 min. Finally, the optical density at 405 nm was measured in a microplate reader. PGE_2 concentrations in the samples were calculated from a PGE_2 standard curve (39.1–5000 pg/ml) which was run in parallel. PGE_2 levels in the supernatant and lysate of control

(untreated) erythrocytes were 92 ± 28 pg per 10^9 cells ($n = 5$) and 26 ± 2 pg per 10^9 cells ($n = 3$), respectively, and were set as 100%. PGE_2 levels in the samples of erythrocytes exposed to hyperosmotic Ringer, Cl^--free extracellular fluid or ionomycin were calculated as % of the appropriate controls.

Immunoblotting

Enriched and washed erythrocytes (0.3%. hematocrit) were incubated at 37°C for 12 or 1 h in NaCl Ringer solution containing PGE_2 (50 μM) or ionomycin (1 μM), respectively. For controls, only vehicle (ethanol) was added to the 12 and 1 h incubations. In further experiments, a mixture of calpain inhibitors I and II (177 and 70 μM, respectively) or ethanol vehicle was pre- (30 min) and coincubated together with PGE_2 or control vehicle. Thereafter, erythrocytes were centrifuged, and the cell pellets (100 μl) hypotonically lysed in 50 ml of 20 mM HEPES/NaOH (pH 7.4) containing a cocktail of protease inhibitors composed of 2.5 mM EDTA, 10 μg/ml pepstatin A, 10 μg/ml leupeptin, 5 μg/ml aprotinin and 0.1 mM phenylmethylsulfonyl fluoride (PMSF) from Roche (Mannheim, Germany). Ghost membranes were pelleted (15 000 rpm for 20 min at 4°C) and resuspended in 10 mM HEPES/NaOH (pH 7.4) containing the protease inhibitor cocktail and re-pelleted. Then, white ghost membranes were solubilized in 125 mM NaCl, 25 mM HEPES/NaOH (pH 7.3), 10 mM EDTA, 10 mM Na-pyrophosphate, 10 mM NaF, 0.1% SDS, 0.5% deoxycholic acid, 1% Triton X-100, and 10 μl β-mercaptoethanol. The protein concentration of the samples was determined using the Bradford method (Biorad, München, Germany) with BSA (Sigma) as standard. Equal amounts of lysate protein (50 μg per lane) were separated by 6% SDS-PAGE, and proteins were transferred to Protan BA83 nitrocellulose membranes (Schleicher and Schuell, Dassel, Germany). Protein transfer was controlled by Ponceau red staining (Figure 4d, e). After blocking with 5% nonfat milk at 4°C overnight, the blots were probed for 1 h at room temperature with a commercial monoclonal mouse anti-human ankyrin R antibody (clone ANK016 produced by EMD Biosciences for Calbiochem, San Diego, CA, USA; 1 : 200 dilution in PBS–0.1% Tween 20–5% nonfat milk) or with a polyclonal rabbit anti-human μ-calpain (domain IV) antibody (Sigma, affinity isolated antibody C5611; 1 : 1000 dilution in PBS-0.1% Tween 20–5% nonfat milk). After washing, the blots were incubated with a secondary sheep anti-mouse or goat anti-rabbit antibody (1 : 1000 dilution each) conjugated with horseradish peroxidase (Amersham, Freiburg, Germany) for 1 h at 21°C. Antibody binding was detected with the enhanced chemiluminescence (ECL) kit (Amersham).

Statistics

Data were expressed as means $\pm$ S.E.M. and statistical analysis was made by ANOVA or unpaired two-tailed *t*-test, as appropriate. $P \leqslant 0.05$ was considered statistically significant.

Acknowledgements

We acknowledge the technical assistance of E. Faber and K. Bauer and the meticulous preparation of the manuscript by Tanja Loch. This study was supported by the Deutsche Forschungsgemeinschaft, Nr. La 315/4-3, La 315/6-1, La 315/11-1 and 11-2, La 315/13-1, Le 792/3-3, the Bundesministerium für Bildung, Wissenschaft, Forschung und Technologie (Center for Interdisciplinary Clinical Research) 01 KS 9602, and the Biomed program of the EU (BMH4-CT96-0602).

References

1. Green DR and Reed JC (1998) Mitochondria and apoptosis. Science 281: 1309–1312
2. Berg CP, Engels IH, Rothbart A, Lauber K, Renz A, Schlosser SF, Schulze-Osthoff K and Wesselborg S (2001) Human mature red blood cells express caspase-3 and caspase-8, but are devoid of mitochondrial regulators of apoptosis. Cell Death Differ. 8: 1197–1206
3. Bratosin D, Estaquier J, Petit F, Arnoult D, Quatannens B, Tissier JP, Slomianny C, Sartiaux C, Alonso C, Huart JJ, Montreuil J and Ameisen JC (2001) Programmed cell death in mature erythrocytes: a model for investigating death effector pathways operating in the absence of mitochondria. Cell Death Differ. 8: 1143–1156
4. Daugas E, Cande C and Kroemer G (2001) Erythrocytes: death of a mummy. Cell Death Differ. 8: 1131–1133
5. Lang KS, Duranton C, Poehlmann H, Myssina S, Bauer C, Lang F, Wieder T and Huber SM (2003) Cation channels trigger apoptotic death of erythorcytes. Cell Death Differ. 10: 249–256
6. Lang KS, Myssina S, Tanneur V, Wieder T, Huber SM, Lang F and Duranton C (2003) Inhibition of erythrocyte cation channels and apoptosis by ethylisopropylamiloride. Naunyn-Schmiedeberg's Arch Pharmacol. 367: 391–396
7. Lang KS, Myssina S, Brand V, Sandu C, Lang PA, Berchtold S, Huber SM, Lang F and Wieder T (2004) Involvement of ceramide in hyperosmotic shock-induced death of erythrocytes. Cell Death Differ. 11: 231–243
8. Gulbins E, Jekle A, Ferlinz K, Grassme H and Lang F (2000) Physiology of apoptosis. Am. J. Physiol. Renal Physiol. 279: F605–F615
9. Dekkers DW, Comfurius P, Bevers EM and Zwaal RF (2002) Comparison between Ca^{2+}-induced scrambling of various fluorescently labelled lipid analogues in red blood cells. Biochem. J. 362: 741–747
10. Woon LA, Holland JW, Kable EP and Roufogalis BD (1999) Ca^{2+} sensitivity of phospholipid scrambling in human red cell ghosts. Cell Calcium 25: 313–320
11. Fadok VA, Bratton DL, Rose DM, Pearson A, Ezekewitz RA and Henson PM (2000) A receptor for phosphatidylserine-specific clearance of apoptotic cells. Nature 405: 85–90
12. Henson PM, Bratton DL and Fadok VA (2001) The phosphatidylserine receptor: a crucial molecular switch? Nat. Rev. Mol. Cell Biol. 2: 627–633
13. Messmer UK and Pfeilschifter J (2000) New insights into the mechanism for clearance of apoptotic cells. BioEssays 22: 878–881
14. Boas FE, Forman L and Beutler E (1998) Phosphatidylserine exposure and red cell viability in red cell aging and in hemolytic anemia. Proc. Natl. Acad. Sci. USA 95: 3077–3081
15. Eda S and Sherman IW (2002) Cytoadherence of malaria-infected red blood cells involves exposure of phosphatidylserine. Cell. Physiol. Biochem. 12: 373–384
16. Lauber K, Bohn E, Krober SM, Xiao YJ, Blumenthal SG, Lindemann RK, Marini P, Wiedig C, Zobywalski A, Baksh S, Xu Y, Autenrieth IB, Schulze-Osthoff K, Belka C, Stuhler G and Wesselborg S (2003) Apoptotic cells induce migration of phagocytes via caspase-3-mediated release of a lipid attraction signal. Cell 113: 717–730
17. Bookchin RM, Ortiz OE and Lew VL (1987) Activation of calcium-dependent potassium channels in deoxygenated sickled red cells. Prog. Clin. Biol. Res. 240: 193–200
18. Brugnara C, de Franceschi L and Alper SL (1993) Inhibition of Ca(2+)-dependent K+ transport and cell dehydration in sickle erythrocytes by clotrimazole and other imidazole derivatives. J. Clin. Invest. 92: 520–526
19. Lang PA, Kaiser S, Myssina S, Wieder T, Lang F and Huber SM (2003) Role of Ca^{2+}-activated K^+ channels in human erythrocyte apoptosis. Am. J. Physiol. Cell. Physiol. 285: C1553–C1560
20. Duranton C, Huber SM and Lang F (2002) Oxidation induces a Cl(–)-dependent cation conductance in human red blood cells. J. Physiol. 539: 847–855
21. Huber SM, Gamper N and Lang F (2001) Chloride conductance and volume-regulatory nonselective cation conductance in human red blood cell ghosts. Pflugers Arch. 441: 551–558
22. Kaestner L and Bernhardt I (2002) Ion channels in the human red blood cell membrane: their further investigation and physiological relevance. Bioelectrochemistry 55: 71–74
23. Kaestner L, Tabellion W, Lipp P and Bernhardt I (2004) Prostaglandin E_2 activates channel−mediated calcium entry in human erythrocytes: An

indication of a blood clot formation supporting process. Thrombosis Haemostasis 92: 1269–1272
24. Allen JE and Rasmussen H (1971) Human red blood cells: prostaglandin E2, epinephrine, and isoproterenol alter deformability. Science 174: 512–514
25. Li Q, Jungmann V, Kiyatkin A and Low PS (1996) Prostaglandin E2 stimulates a Ca^{2+}-dependent K^+ channel in human erythrocytes and alters cell volume and filterability. J. Biol. Chem. 271: 18651–18656
26. Bratosin D, Leszczynski S, Sartiaux C, Fontaine O, Descamps J, Huart JJ, Poplineau J, Goudaliez F, Aminoff D and Montreuil J (2001) Improved storage of erythrocytes by prior leukodepletion: flow cytometric evaluation of stored erythrocytes. Cytometry 46: 351–356
27. Lopes AG, Soares AC, Santos DP, Fernandes MS, Leao-Ferreira LR, Quintana-Gomes E and Caruso-Neves C (2004) PLA2/PGE2 are involved in the inhibitory effect of bradykinin on the angiotensin-(1–7)-stimulated Na(+)-ATPase activity of the proximal tubule. Regul. Pept. 117: 37–41
28. Lang F, Busch GL, Ritter M, Völkl H, Waldegger S, Gulbins E and Häussinger D (1998) Functional significance of cell volume regulatory mechanisms. Physiol. Rev. 78: 247–306
29. Michea L, Ferguson DR, Peters EM, Andrews PM, Kirby MR and Burg MB (2000) Cell cycle delay and apoptosis are induced by high salt and urea in renal medullary cells. Am. J. Physiol. Renal Physiol. 278: F209–F218
30. Rosette C and Karin M (1996) Ultraviolet light and osmotic stress: activation of the JNK cascade through multiple growth factor and cytokine receptors. Science 274: 1194–1197
31. Duranton C, Huber S, Tanneur V, Lang K, Brand V, Sandu C and Lang F (2003) Electrophysiological properties of the *Plasmodium falciparum*-induced cation conductance of human erythrocytes. Cell. Physiol. Biochem. 13: 189–198
32. Franco RS, Palascak M, Thompson H, Rucknagel DL and Joiner CH (1996) Dehydration of transferrin receptor-positive sickle reticulocytes during continuous or cyclic deoxygenation: role of KCl cotransport and extracellular calcium. Blood 88: 4359–4365
33. Yang T, Park JM, Arend L, Huang Y, Topaloglu R, Pasumarthy A, Praetorius H, Spring K, Briggs JP and Schnermann J (2000) Low chloride stimulation of prostaglandin E2 release and cyclooxygenase-2 expression in a mouse macula densa cell line. J. Biol. Chem. 275: 37922–37929
34. Oonishi T, Sakashita K, Ishioka N, Suematsu N, Shio H and Uyesaka N (1998) Production of prostaglandins E1 and E2 by adult human red blood cells. Prostagland. Other Lipid Mediat. 56: 89–101
35. Brugnara C, de Franceschi L and Alper SL (1993) Ca(2+)-activated K+ transport in erythrocytes. Comparison of binding and transport inhibition by scorpion toxins. J. Biol. Chem. 268: 8760–8768
36. Brugnara C, Armsby CC, Sakamoto M, Rifai N, Alper SL and Platt O (1995) Oral administration of clotrimazole and blockade of human erythrocyte Ca(++)-activated K+ channel: the imidazole ring is not required for inhibitory activity. J. Pharmacol. Exp. Ther. 273: 266–272
37. Bortner CD, Hughes Jr FM and Cidlowski JA (1997) A primary role for K^+ and Na^+ efflux in the activation of apoptosis. J. Biol. Chem. 272: 32436–32442
38. Bortner CD and Cidlowski JA (1999) Caspase independent/dependent regulation of K(+), cell shrinkage, and mitochondrial membrane potential during lymphocyte apoptosis. J. Biol. Chem. 274: 21953–21962
39. Gomez-Angelats M, Bortner CD and Cidlowski JA (2000) Protein kinase C (PKC) inhibits fas receptor-induced apoptosis through modulation of the loss of K^+ and cell shrinkage. A role for PKC upstream of caspases. J. Biol. Chem. 275: 19609–19619
40. Hughes Jr FM, Bortner CD, Purdy GD and Cidlowski JA (1997) Intracellular K^+ suppresses the activation of apoptosis in lymphocytes. J. Biol. Chem. 272: 30567–30576
41. Hughes Jr FM and Cidlowski JA (1999) Potassium is a critical regulator of apoptotic enzymes *in vitro* and *in vivo*. Adv. Enzyme Regul. 39: 157–171
42. Montague JW, Bortner CD, Hughes Jr FM and Cidlowski JA (1999) A necessary role for reduced intracellular potassium during the DNA degradation phase of apoptosis. Steroids 64: 563–569
43. Perez GI, Maravei DV, Trbovich AM, Cidlowski JA, Tilly JL and Hughes Jr FM. (2000) Identification of potassium-dependent and -independent components of the apoptotic machinery in mouse ovarian germ cells and granulosa cells. Biol. Reprod. 63: 1358–1369
44. Romero PJ and Romero EA (1999) Effect of cell ageing on Ca^{2+} influx into human red cells. Cell Calcium 26: 131–137
45. Siegel DL, Goodman SR and Branton D (1980) The effect of endogenous proteases on the spectrin binding proteins of human erythrocytes. Biochim. Biophys. Acta 598: 517–527
46. Hall TG and Bennett V (1987) Regulatory domains of erythrocyte ankyrin. J. Biol. Chem. 262: 10537–10545
47. Mandal D, Moitra PK, Saha S and Basu J (2002) Caspase 3 regulates phosphatidylserine externalization and phagocytosis of oxidatively stressed erythrocytes. FEBS Lett. 513: 184–188
48. Mandal D, Baudin-Creuza V, Bhattacharyya A, Pathak S, Delaunay J, Kundu M and Basu J (2003) Caspase 3-mediated proteolysis of the *N*-terminal cytoplasmic domain of the human erythroid anion exchanger 1 (band 3). J. Biol. Chem. 278: 52551–52558
49. Kiefer CR and Snyder LM (2000) Oxidation and erythrocyte senescence. Curr. Opin. Hematol. 7: 113–116
50. Damonte G, Guida L, Sdraffa A, Benatti U, Melloni E, Forteleoni G, Meloni T, Carafoli E and De Flora A (1992) Mechanisms of perturbation of erythrocyte calcium homeostasis in favism. Cell Calcium 13: 649–658
51. Lang KS, Myssina S, Lang PA, Tanneur V, Kempe DS, Huber SM, Wieder T, Lang F and Duranton C (2004) Inhibition of erythrocyte phosphatidylserine exposure by urea and Cl^-. Am. J. Physiol. Renal Physiol. 286: F1046–F1053
52. Mason J (1986) The pathophysiology of ischaemic acute renal failure. A new hypothesis about the initiation phase. Renal Physiol. 9: 129–147
53. Joiner CH (1993) Cation transport and volume regulation in sickle red blood cells. Am. J. Physiol. 264: C251–C270
54. Mach-Pascual S, Darbellay R, Pilotto PA and Beris P (1996) Investigation of microcytosis: a comprehensive approach. Eur. J. Haematol. 57: 54–61
55. Jolobe OM (2000) Prevalence of hypochromia (without microcytosis) *vs* microcytosis (without hypochromia) in iron deficiency. Clin. Lab. Haematol. 22: 79–80
56. Lang KS, Roll B, Myssina S, Schittenhelm M, Scheel-Walter HG, Kanz L, Fritz J, Lang F, Huber SM and Wieder T (2002) Enhanced erythrocyte apoptosis in sickle cell anemia, thalassemia and glucose-6-phosphate dehydrogenase deficiency. Cell. Physiol. Biochem. 12: 365–372
57. Hellem AJ (1960) The adhesiveness of human blood platelets *in vitro*. Scand. J. Clin. Lab. Invest. 12 (Suppl): 1–117
58. Hellem AJ, Borchgrevink CF and Ames SB (1961) The role of red cells in haemostasis: the relation between haematocrit, bleeding time and platelet adhesiveness. Br. J. Haematol. 7: 42–50
59. Santos MT, Valles J, Marcus AJ, Safier LB, Broekman MJ, Islam N, Ullman HL, Eiroa AM and Aznar J (1991) Enhancement of platelet reactivity and modulation of eicosanoid production by intact erythrocytes. A new approach to platelet activation and recruitment. J. Clin. Invest. 87: 571–580
60. Valles J, Santos MT, Aznar J, Marcus AJ, Martinez-Sales V, Portoles M, Broekman MJ and Safier LB (1991) Erythrocytes metabolically enhance collagen-induced platelet responsiveness via increased thromboxane production, adenosine diphosphate release, and recruitment. Blood 78: 154–162
61. Laufer S (2003) Role of eicosanoids in structural degradation in osteoarthritis. Curr. Opin. Rheumatol. 15: 623–627
62. Cabado AG, Vieytes MR and Botana LM (1994) Effect of ion composition on the changes in membrane potential induced with several stimuli in rat mast cells. J. Cell. Physiol. 158: 309–316
63. Gamper N, Huber SM, Badawi K and Lang F (2000) Cell volume-sensitive sodium channels upregulated by glucocorticoids in U937 macrophages. Pflugers Arch. 441: 281–286
64. Koch J and Korbmacher C (1999) Osmotic shrinkage activates nonselective cation (NSC) channels in various cell types. J. Membr. Biol. 168: 131–139
65. Volk T, Fromter E and Korbmacher C (1995) Hypertonicity activates nonselective cation channels in mouse cortical collecting duct cells. Proc. Natl. Acad. Sci. USA 92: 8478–8482
66. Wehner F, Sauer H and Kinne RK (1995) Hypertonic stress increases the Na^+ conductance of rat hepatocytes in primary culture. J. Gen. Physiol. 105: 507–535
67. Wehner F, Böhmer C, Heinzinger H, van den BF and Tinel H (2000) The hypertonicity-induced Na(+) conductance of rat hepatocytes: physiological significance and molecular correlate. Cell. Physiol. Biochem. 10: 335–340
68. Berridge MJ, Lipp P and Bootman MD (2000) The versatility and universality of calcium signalling. Nat. Rev. Mol. Cell Biol. 1: 11–21
69. Maeno E, Ishizaki Y, Kanaseki T, Hazama A and Okada Y (2000) Normotonic cell shrinkage because of disordered volume regulation is an early prerequisite to apoptosis. Proc. Natl. Acad. Sci. USA 97: 9487–9492

70. Roger F, Martin PY, Rousselot M, Favre H and Feraille E (1999) Cell shrinkage triggers the activation of mitogen-activated protein kinases by hypertonicity in the rat kidney medullary thick ascending limb of the Henle's loop. Requirement of p38 kinase for the regulatory volume increase response. J. Biol. Chem. 274: 34103–34110
71. Hamill OP, Marty A, Neher E, Sakmann B and Sigeorth FJ (1981) Improved patch-clamp techniques for high-resolution current recording from cells and cell-free membrane patches. Pflügers Arch. 391: 85–100
72. Barry PH and Lynch JW (1991) Liquid junction potentials and small cell effects in patch-clamp analysis. J. Membr. Biol. 121: 101–117
73. Andree HA, Reutelingsperger CP, Hauptmann R, Hemker HC, Hermens WT and Willems GM (1990) Binding of vascular anticoagulant alpha (VAC alpha) to planar phospholipid bilayers. J. Biol. Chem. 265: 4923–4928
74. Andrews DA, Yang L and Low PS (2002) Phorbol ester stimulates a protein kinase C-mediated agatoxin-TK-sensitive calcium permeability pathway in human red blood cells. Blood 100: 3392–3399